CONJUGATE AUGMENTED SPATIAL-TEMPORAL NEAR-FIELD SOURCES LOCALIZATION WITH CROSS ARRAY

Zhiwei Jiang[1], *Hua Chen*[1,*], *Wei Liu*[2], *Ye Tian*[1] *and Gang Wang*[1]

[1]Faculty of Electrical Engineering and Computer Science, Ningbo University, Ningbo 315211, China.
[2]Department of Electronic and Electrical Engineering, University of Sheffield, Sheffield S1 3JD, UK.
Email: dkchenhua0714@hotmail.com

ABSTRACT

A new near-field source localization method is proposed for two-dimensional (2-D) direction-of-arrival (DOA) and range estimation based on a symmetrical cross array. It first employs the conjugate symmetry property of the signal autocorrelation at different time delays to construct a conjugate augmented spatial-temporal cross correlation matrix, then the extended steering vector is decoupled to avoid the usual multiple-dimensional (M-D) search based on the properties of the Khatri-Rao product, and finally three one-dimensional (1-D) MUSIC type searches are employed to obtain the results. The proposed method can realize automatic pairing of multiple parameters associated with each source and it also works in the underdetermined case.

***Index Terms*—** Near-field, spatial-temporal, source localization, cross array, automatic pairing

1. INTRODUCTION

Source localization is an important research problem in array signal processing, and it has a wide range of applications such as radar, sonar and wireless communications [1, 2]. Many efforts have been devoted to localization of FF sources, such as the subspace based methods [3, 4] and the sparsity based methods [5, 6]. However, these high resolution DOA estimation methods are not directly applicable to the case with NF sources, as the propagation delay of NF sources, utilizing Fresnel approximation [7], varies quadratically with respect to sensor locations. Several methods [8–12] have been proposed to perform NF sources localization; however, one common limitation for these methods is that they are only focused on the problem of 2-D parameter estimation for NF sources, namely azimuth and range. In the three-dimensional (3-D) NF source model, the estimated parameters include not only the azimuth and range, but also the elevation, thus leading to an even more complicated parameter pairing problem. Although several methods have been reported for localization of NF sources using the spherical coordinates system (azimuth, elevation, and range), they are only efficacious in the case of overdetermined or single source estimation [13–15]. Moreover, two cumulant based localization methods are introduced for 3-D NF sources in [16, 17]. Although the algorithms proposed in [10, 12] can also be directly extended to the 3-D NF source case, they require more array sensors than the number of sources.

In this paper, a conjugate augmented spatial-temporal localization method for NF sources is proposed employing a cross array. We first use the spatial-temporal characteristics of the array received data and the conjugate symmetry property of signal autocorrelation function to increase the degrees of freedom, and then use the properties of the Khatri-Rao product and the 1-D MUSIC algorithm to obtain the estimated angle and range, which can be automatically paired in the underdetermined case.

Notations: Matrices and vectors are denoted by boldfaced capital letters and lower-case letters, respectively. For an integer M, $[M]$ is defined as the set $\{\ -M, \cdots\ , 0, \cdots\ ,\ \ M\ \}$. $|\cdot|$ denotes the absolute value of a scalar or cardinality of a set. The superscript $(\cdot)^T, (\cdot)^*, (\cdot)^H$ stand for transpose, conjugate and conjugate transpose, respectively. The notations $E\{\cdot\}, \delta(), \otimes, \odot, \mathbf{I}_D, \mathbf{J}_D, \det[\cdot]$ represent the statistical expectation, Dirac function, Kronecker product, Khatri-Rao (KR) product, the $D \times D$ identity matrix, the $D \times D$ exchange matrix with ones on its antidiagonal and zeros elsewhere, and determinant, respectively. $diag\{\mathbf{Z}\}$ represents diagonal elements of the matrix $\mathbf{Z}$.

2. SIGNAL MODEL

As shown in Fig. 1, there are K NF, narrowband, spatially and temporally uncorrelated sources $\{s_k(n)\}_{k=1}^K$ ($n = 1, 2, ..., N$, where N denotes the number of snapshots) impinging onto a symmetric cross array consisting of two uniform linear arrays (ULAs). The ULA on x-axis is denoted as array $\boldsymbol{x}$, whose element indices are $[M_x] =$

This work was supported by the National Natural Science Foundation of China under Grants 62001256, the Key Laboratory of Intelligent Perception and Advanced Control of State Ethnic Affairs Commission under Grant MD-IPAC-2019102, the Zhejiang Provincial Natural Science Foundation of China under Grant LR20F010001, and the UK Engineering and Physical Sciences Research Council (EPSRC) under grants EP/T517215/1 and EP/V009419/1.

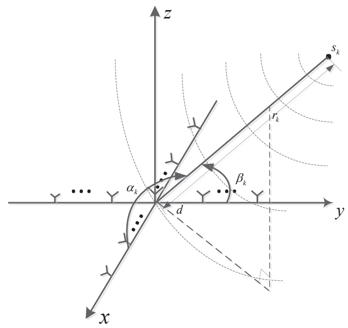

Fig. 1. 3-D localization configuration for NF sources.

$\{ -M_x, \cdots, M_x \}$ and the total number of sensors is given by $N_x = |[M_x]|$. Similarly, the ULA on y-axis is represented as array $\boldsymbol{y}$, whose indices are denoted as $[M_y] = \{ -M_y, \cdots, M_y \}$ and its number of sensors is $N_y = |[M_y]|$. The element spacing of each array is d ($d \leq \lambda/4$, where λ denotes signal wavelength). In Fig. 1, let α_k and β_k denote the angles between the k-th signal and the $\boldsymbol{x}$ and $\boldsymbol{y}$ axes, respectively, and the array center be the phase reference point; then the signals received by the two ULAs can be written in a more compact form as follows,

$$\mathbf{x}(n) = \mathbf{A}_x\mathbf{s}(n) + \mathbf{n}_x(n) \tag{1}$$

$$\mathbf{y}(n) = \mathbf{A}_y\mathbf{s}(n) + \mathbf{n}_y(n), \tag{2}$$

where $\mathbf{x}(n)$ and $\mathbf{y}(n)$ denote the output vectors of array $\boldsymbol{x}$ and array $\boldsymbol{y}$, respectively; With the Fresnel approximation in [17], $\mathbf{A}_x = [\mathbf{a}(\omega_{x1}, \phi_{x1}), ..., \mathbf{a}(\omega_{xk}, \phi_{xk})]$ with $\mathbf{a}(\omega_{xk}, \phi_{xk}) = [e^{-j[\omega_{xk}(-M_x) + \phi_{xk}(-M_x)^2]}, \cdots, e^{-j(\omega_{xk}M_x + \phi_{xk}M_x{}^2)}]^T$ denotes the manifold matrix of array $\boldsymbol{x}$, and $\mathbf{A}_y$ is similarly defined, where

$$\begin{aligned} \omega_{xk} &= -\tfrac{2\pi d}{\lambda}\cos\alpha_k, \phi_{xk} = \tfrac{\pi d^2}{\lambda r_k}\sin^2\alpha_k \\ \omega_{yk} &= -\tfrac{2\pi d}{\lambda}\cos\beta_k, \phi_{yk} = \tfrac{\pi d^2}{\lambda r_k}\sin^2\beta_k, \end{aligned} \tag{3}$$

$\mathbf{n}_x(n)$ and $\mathbf{n}_y(n)$ represent the additive Gaussian noise vectors for the two ULAs, respectively.

Since ω_{xk} and ϕ_{xk} are only related to α_k and r_k, $\mathbf{a}(\omega_{xk}, \phi_{xk})$ is simplified into $\mathbf{a}_x(\alpha_k, r_k)$ in the following derivations and similarly, $\mathbf{a}(\omega_{yk}, \phi_{yk})$ is simplified into $\mathbf{a}_y(\beta_k, r_k)$.

3. PROPOSED METHOD

In order to make full use of the spatial-temporal 2-D characteristics, $\mathbf{x}(n)$ and $\mathbf{y}(n)$ are divided into L frames according to the principle of maximum overlap in the time domain [18]. The l-th ($l = 1, 2, \cdots, L$) frame data can be expressed as:

$$\begin{aligned} \mathbf{X}_l &= [\mathbf{x}(l), \mathbf{x}(l+1), \cdots, \mathbf{x}(l+N-L)] \\ \mathbf{Y}_l &= [\mathbf{y}(l), \mathbf{y}(l+1), \cdots, \mathbf{y}(l+N-L)] \end{aligned} \tag{4}$$

With the array signal model described in Section 2, the delay cross-correlation item of measured data $\mathbf{x}(n)$ and $\mathbf{y}(n)$ satisfies the following relationship

$$\begin{aligned} & r_{m_1,m_2}(l-1+L) \\ &= E\{x_{m_1}(n+l-1)y^*_{m_2}(n)\} \\ &= \sum_{k_1=1}^{K} [a_{x,m_1}(\alpha_{k_1}, r_{k_1})a^*_{y,m_2}(\beta_{k_1}, r_{k_1}) \\ &\quad \times \mathbf{R}_{ss}(k_1, l-1+L)] + \delta(m_1)\delta(m_2)\delta(l-1)\sigma_w^2 \end{aligned} \tag{5}$$

$$\begin{aligned} & r_{m_1,m_2}(-(l-1)+L) \\ &= E\{x_{m_1}(n)y^*_{m_2}(n+l-1)\} \\ &= \sum_{k_1=1}^{K} [a_{x,m_1}(\alpha_{k_1}, r_{k_1})a^*_{y,m_2}(\beta_{k_1}, r_{k_1}) \\ &\quad \times \mathbf{R}_{ss}(k_1, -(l-1)+L)] + \delta(m_1)\delta(m_2)\delta(l-1)\sigma_w^2 \end{aligned} \tag{6}$$

where $m_1 = -M_x, \cdots, 0, \cdots, M_x, m_2 = -M_y, \cdots, 0, \cdots, M_y, l = 1, 2, \cdots, L, \sigma_w^2$ denotes the noise power, $\mathbf{R}_{ss}(k_1, l_1)$ represents the entry at the k_1-th row and l_1-th ($l_1 = 1, 2, \cdots, 2L-1$) column of the signal delay autocorrelation matrix $\mathbf{R}_{ss}$, $\mathbf{R}_{ss}(:, l_1) = diag\{E\{\mathbf{S}_{l+l_1-L}\mathbf{S}_l^H\}\}$, $\mathbf{S}_l = [\mathbf{s}(l), \mathbf{s}(l+1), \cdots, \mathbf{s}(l+N-L)]$.

By arranging $r_{m_1,m_2}(l_1)(l_1 = 1, 2, \cdots, 2L-1)$, we have

$$\tilde{\mathbf{R}} = E\left\{\tilde{\mathbf{R}}_{xy}\tilde{\mathbf{R}}_{xy}^H\right\} = \tilde{\mathbf{A}}_{xy}\tilde{\mathbf{R}}_s\tilde{\mathbf{A}}_{xy}^H + \sigma_w^4\tilde{\mathbf{R}}_w \tag{7}$$

where $\mathbf{r}_{xy}(l_1) = [r_{-M_x,-M_y}(l_1), \cdots, r_{M_x,-M_y}(l_1), \cdots, r_{-M_x,M_y}(l_1), \cdots, r_{M_x,M_y}(l_1)]^T$. Note that there is only one nonzero element in $\mathbf{R}_{w0}$, that is, $\mathbf{R}_{w0}(\frac{N_xN_y+1}{2}, L) = 1$.

Due to the conjugate symmetry property of the signal autocorrelation function [18], we can have the following expressions

$$\begin{aligned} & \mathbf{r}^*_{xy}(l_2+L) \\ &= [(\mathbf{A}^*_y(\beta, r) \odot \mathbf{A}_x(\alpha, r))\mathbf{R}_{ss}(:, l_2+L)]^* + \sigma_w^2\delta(l_2)\mathbf{r}_{w0} \\ &= [(\mathbf{A}_y(\beta, r) \odot \mathbf{A}^*_x(\alpha, r))\mathbf{R}_{ss}(:, L-l_2)] + \sigma_w^2\delta(l_2)\mathbf{r}_{w0} \end{aligned} \tag{8}$$

$$\begin{aligned} & \mathbf{r}^*_{xy}(L-l_2) \\ &= [(\mathbf{A}^*_y(\beta, r) \odot \mathbf{A}_x(\alpha, r))\mathbf{R}_{ss}(:, L-l_2)]^* + \sigma_w^2\delta(l_2)\mathbf{r}_{w0} \\ &= [(\mathbf{A}_y(\beta, r) \odot \mathbf{A}^*_x(\alpha, r))\mathbf{R}_{ss}(:, l_2+L)] + \sigma_w^2\delta(l_2)\mathbf{r}_{w0} \end{aligned} \tag{9}$$

where $l_2 = 1, 2, \cdots, L-1$ and $\mathbf{r}_{w0} = [0, \ldots, 1, \ldots, 0]$.

By combining equations from (11) to (9), the following conjugate augmented cross-correlation matrix can be constructed

$$\begin{aligned} \tilde{\mathbf{R}}_{xy} &= \begin{bmatrix} \mathbf{R}_{xy} \\ \mathbf{R}^*_{xy}\mathbf{J}_{(2L-1)} \end{bmatrix} \\ &= \begin{bmatrix} \mathbf{A}^*_y(\beta, r) \odot \mathbf{A}_x(\alpha, r) \\ \mathbf{A}_y(\beta, r) \odot \mathbf{A}^*_x(\alpha, r) \end{bmatrix} \mathbf{R}_{ss} + \sigma_w^2 \begin{bmatrix} \mathbf{R}_{w0} \\ \mathbf{R}_{w0}\mathbf{J}_{(2L-1)} \end{bmatrix} \\ &= \tilde{\mathbf{A}}_{xy}\mathbf{R}_{ss} + \sigma_w^2\tilde{\mathbf{R}}_{w0} \end{aligned} \tag{10}$$

Then, calculate the covariance matrix of $\tilde{\mathbf{R}}_{xy}$ as

$$\tilde{\mathbf{R}}=E\left\{\tilde{\mathbf{R}}_{xy}\tilde{\mathbf{R}}_{xy}^H\right\}=\tilde{\mathbf{A}}_{xy}\tilde{\mathbf{R}}_s\tilde{\mathbf{A}}_{xy}^H+\sigma_w^4\tilde{\mathbf{R}}_w \tag{11}$$

where $\tilde{\mathbf{R}}_s=E\left\{\mathbf{R}_{ss}\mathbf{R}_{ss}^H\right\}$ is the covariance matrix of signal autocorrelation matrix $\mathbf{R}_{ss}$, and $\tilde{\mathbf{R}}_w$ is extremely sparse, with only $\tilde{\mathbf{R}}_w(\frac{N_xN_y+1}{2},\frac{N_xN_y+1}{2})=1$.

Performing eigenvalue decomposition (EVD) on $\tilde{\mathbf{R}}$, we obtain:

$$\tilde{\mathbf{R}}=\mathbf{U}_s\mathbf{\Sigma}_s\mathbf{U}_s^H+\mathbf{U}_n\mathbf{\Sigma}_n\mathbf{U}_n^H \tag{12}$$

where $\mathbf{U}_s$ and $\mathbf{U}_n$ are signal subspace and noise subspace, respectively, and $\mathbf{\Sigma}_s$ and $\mathbf{\Sigma}_n$ are the corresponding diagonal eigenvalue matrices.

According to the relationship between Khatri-Rao product and Kronecker product, (11) can be rewritten as:

$$\begin{aligned}&\mathbf{R}_{xy}\\&=[\mathbf{a}_y^*(\beta_1,r_1)\otimes\mathbf{a}_x(\alpha_1,r_1),\cdots,\mathbf{a}_y^*(\beta_K,r_K)\otimes\mathbf{a}_x(\alpha_K,r_K)]\\&\quad\times\mathbf{R}_{ss}+\sigma_w^2\mathbf{R}_{w0}\end{aligned} \tag{13}$$

For simplicity, $\mathbf{a}_x(\alpha,r)$, $\mathbf{a}_y(\beta,r)$ and $\tilde{\mathbf{a}}_{xy}$ represent an arbitrary column vector of $\mathbf{A}_x$, $\mathbf{A}_y$ and $\tilde{\mathbf{R}}_{xy}$ respectively. According to the symmetry of array structure, $\mathbf{a}_y^*(\beta,r)$ can be decomposed into the following form [11, 19]:

$$\begin{aligned}&\mathbf{a}_y^*(\beta,r)\\&=\begin{bmatrix}e^{j(-M_y)\omega_y}&&&\\&e^{j(-M_y+1)\omega_y}&&\\&&\ddots&\\&&&1\\&&\iddots&\\&e^{j(M_y-1)\omega_y}&&\\e^{jM_y\omega_y}&&&\end{bmatrix}\begin{bmatrix}e^{j(-M_y)^2\phi_y}\\e^{j(-M_y+1)^2\phi_y}\\\vdots\\e^{j(-1)^2\phi_y}\\1\end{bmatrix}\\&=\boldsymbol{\zeta}_y^*(\beta)\boldsymbol{\upsilon}_y^*(\beta,r)\end{aligned} \tag{14}$$

Then, $\mathbf{a}_y^*(\beta,r)\otimes\mathbf{a}_x(\alpha,r)$ can be rewritten as:

$$\mathbf{a}_y^*(\beta,r)\otimes\mathbf{a}_x(\alpha,r)=(\boldsymbol{\zeta}_y^*(\beta)\boldsymbol{\upsilon}_y^*(\beta,r))\otimes(\mathbf{I}_{N_x}\mathbf{a}_x(\alpha,r)) \tag{15}$$

Similarly,

$$\mathbf{a}_y(\beta,r)\otimes\mathbf{a}_x^*(\alpha,r)=(\boldsymbol{\zeta}_y(\beta)\boldsymbol{\upsilon}_y(\beta,r))\otimes(\mathbf{I}_{N_x}\mathbf{a}_x^*(\alpha,r)) \tag{16}$$

Therefore,

$$\tilde{\mathbf{a}}_{xy}=\begin{bmatrix}(\boldsymbol{\zeta}_y^*(\beta)\boldsymbol{\upsilon}_y^*(\beta,r))\otimes(\mathbf{I}_{N_x}\mathbf{a}_x(\alpha,r))\\(\boldsymbol{\zeta}_y(\beta)\boldsymbol{\upsilon}_y(\beta,r))\otimes(\mathbf{I}_{N_x}\mathbf{a}_x^*(\alpha,r))\end{bmatrix} \tag{17}$$

According to the property of the Kronecker product, we have

$$(\mathbf{A}\otimes\mathbf{B})(\mathbf{C}\otimes\mathbf{D})=\mathbf{AC}\otimes\mathbf{BD} \tag{18}$$

(17) can be rewritten as follows

$$\begin{aligned}\tilde{\mathbf{a}}_{xy}&=\begin{bmatrix}(\boldsymbol{\zeta}_y^*(\beta)\boldsymbol{\upsilon}_y^*(\beta,r))\otimes(\mathbf{I}_{N_x}\mathbf{a}_x(\alpha,r))\\(\boldsymbol{\zeta}_y(\beta)\boldsymbol{\upsilon}_y(\beta,r))\otimes(\mathbf{I}_{N_x}\mathbf{a}_x^*(\alpha,r))\end{bmatrix}\\&=\begin{bmatrix}(\boldsymbol{\zeta}_y^*(\beta)\otimes\mathbf{I}_{N_x})(\boldsymbol{\upsilon}_y^*(\beta,r)\otimes\mathbf{a}_x(\alpha,r))\\(\boldsymbol{\zeta}_y(\beta)\otimes\mathbf{I}_{N_x})(\boldsymbol{\upsilon}_y(\beta,r)\otimes\mathbf{a}_x^*(\alpha,r))\end{bmatrix}\\&=\begin{bmatrix}\mathbf{C}_1(\beta)(\boldsymbol{\upsilon}_y^*(\beta,r)\otimes\mathbf{a}_x(\alpha,r))\\\mathbf{C}_2(\beta)(\boldsymbol{\upsilon}_y(\beta,r)\otimes\mathbf{a}_x^*(\alpha,r))\end{bmatrix}\\&=\begin{bmatrix}\mathbf{C}_1(\beta)&\\&\mathbf{C}_2(\beta)\end{bmatrix}\begin{bmatrix}(\boldsymbol{\upsilon}_y^*(\beta,r)\otimes\mathbf{a}_x(\alpha,r))\\(\boldsymbol{\upsilon}_y(\beta,r)\otimes\mathbf{a}_x^*(\alpha,r))\end{bmatrix}\end{aligned} \tag{19}$$

We define $\mathbf{C}(\beta)$ that is only related to β:

$$\mathbf{C}(\beta)=\begin{bmatrix}\mathbf{C}_1(\beta)&\\&\mathbf{C}_2(\beta)\end{bmatrix} \tag{20}$$

Based on the rank reduction principle [19–21], we can construct the MUSIC spectral function related to angle β:

$$\mathbf{D}(\beta)=\mathbf{C}^H(\beta)\mathbf{U}_n\mathbf{U}_n^H\mathbf{C}(\beta) \tag{21}$$

With (21), an estimator about β can be obtained:

$$\hat{\beta}=\arg\max_{\beta}\frac{1}{\det[\mathbf{D}(\beta)]} \tag{22}$$

With the same operation as (14), $\mathbf{a}_x(\alpha,r)$ can be decomposed into:

$$\mathbf{a}_x(\alpha,r)=\boldsymbol{\zeta}_x(\alpha)\boldsymbol{\upsilon}_x(\alpha,r) \tag{23}$$

We rewrite equation (19) as:

$$\begin{aligned}&\tilde{\mathbf{a}}_{xy}\\&=\begin{bmatrix}\mathbf{C}_1(\beta)&\\&\mathbf{C}_2(\beta)\end{bmatrix}\begin{bmatrix}(\boldsymbol{\upsilon}_y^*(\beta,r)\otimes\mathbf{a}_x(\alpha,r))\\(\boldsymbol{\upsilon}_y(\beta,r)\otimes\mathbf{a}_x^*(\alpha,r))\end{bmatrix}\\&=\begin{bmatrix}\mathbf{C}_1(\beta)&\\&\mathbf{C}_2(\beta)\end{bmatrix}\\&\quad\times\begin{bmatrix}(\mathbf{I}_{M_y+1}\boldsymbol{\upsilon}_y^*(\beta,r)\otimes\boldsymbol{\zeta}_x(\alpha)\boldsymbol{\upsilon}_x(\alpha,r))\\(\mathbf{I}_{M_y+1}\boldsymbol{\upsilon}_y(\beta,r)\otimes\boldsymbol{\zeta}_x^*(\alpha)\boldsymbol{\upsilon}_x^*(\alpha,r))\end{bmatrix}\\&=\begin{bmatrix}\mathbf{C}_1(\beta)&\\&\mathbf{C}_2(\beta)\end{bmatrix}\\&\quad\times\begin{bmatrix}(\mathbf{I}_{M_y+1}\otimes\boldsymbol{\zeta}_x(\alpha))(\boldsymbol{\upsilon}_y^*(\beta,r)\otimes\boldsymbol{\upsilon}_x(\alpha,r))\\(\mathbf{I}_{M_y+1}\otimes\boldsymbol{\zeta}_x^*(\alpha))(\boldsymbol{\upsilon}_y(\beta,r)\otimes\boldsymbol{\upsilon}_x^*(\alpha,r))\end{bmatrix}\\&=\begin{bmatrix}\mathbf{C}_1(\beta)&\\&\mathbf{C}_2(\beta)\end{bmatrix}\begin{bmatrix}\mathbf{E}_1(\alpha)(\boldsymbol{\upsilon}_y^*(\beta,r)\otimes\boldsymbol{\upsilon}_x(\alpha,r))\\\mathbf{E}_2(\alpha)(\boldsymbol{\upsilon}_y(\beta,r)\otimes\boldsymbol{\upsilon}_x^*(\alpha,r))\end{bmatrix}\\&=\begin{bmatrix}\mathbf{C}_1(\beta)&\\&\mathbf{C}_2(\beta)\end{bmatrix}\begin{bmatrix}\mathbf{E}_1(\alpha)&\\&\mathbf{E}_2(\alpha)\end{bmatrix}\\&\quad\times\begin{bmatrix}(\boldsymbol{\upsilon}_y^*(\beta,r)\otimes\boldsymbol{\upsilon}_x(\alpha,r))\\(\boldsymbol{\upsilon}_y(\beta,r)\otimes\boldsymbol{\upsilon}_x^*(\alpha,r))\end{bmatrix}\end{aligned} \tag{24}$$

Define $\mathbf{E}(\alpha)$ that is only related to α:

$$\mathbf{E}(\alpha)=\begin{bmatrix}\mathbf{E}_1(\alpha)&\\&\mathbf{E}_2(\alpha)\end{bmatrix} \tag{25}$$

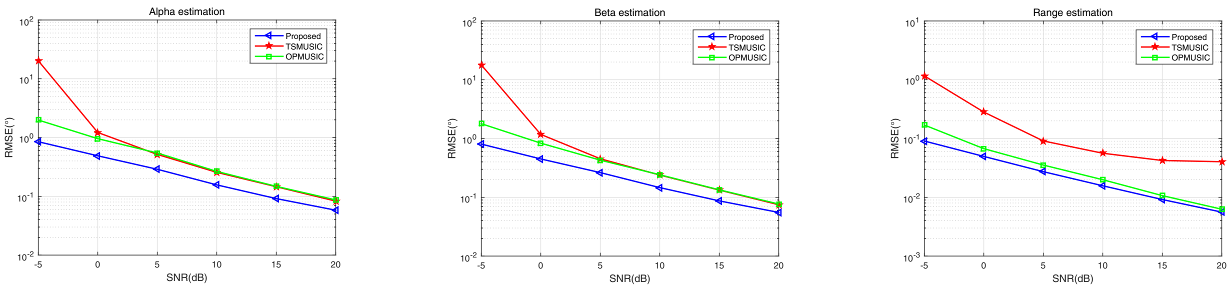

(a) RMSE-alpha (b) RMSE-beta (c) RMSE-r

Fig. 2. RMSE versus SNR.

Based on (25), we can construct another MUSIC spectral function for angle α:

$$\mathbf{F}(\hat{\beta}, \alpha) = \mathbf{E}^H(\alpha)\mathbf{C}^H(\hat{\beta})\mathbf{U}_n\mathbf{U}_n^H\mathbf{C}(\hat{\beta})\mathbf{E}(\alpha) \tag{26}$$

Substituting the estimated parameter $\hat{\beta}$ into $\mathbf{F}(\hat{\beta}, \alpha)$, another estimator in regard to the angle parameter $\hat{\alpha}$ can be obtained:

$$\hat{\alpha} = \arg\max_{\alpha} \frac{1}{\det[\mathbf{F}(\hat{\beta}, \alpha)]} \tag{27}$$

After obtaining the angle parameters of NF sources according to (22) and (27), substitute $\hat{\alpha}, \hat{\beta}$ into the classical MUSIC spectral function to construct the spectral peak search function about the range parameter r as follows:

$$\hat{r}_k = \arg\max_{r} f(\hat{\alpha}_k, \hat{\beta}_k, r) = \frac{1}{\tilde{\mathbf{a}}_{xy}^H(\hat{\alpha}, \hat{\beta}, r)\mathbf{U}_n\mathbf{U}_n^H\tilde{\mathbf{a}}_{xy}(\hat{\alpha}, \hat{\beta}, r)} \tag{28}$$

4. SIMULATION RESULTS

Table 1. Summary of results

$\alpha_k(^\circ)$		$\beta_k(^\circ)$		$r_k(\lambda)$	
True	Estimated	True	Estimated	True	Estimated
20	20.1300	35	35.0400	0.2000	0.1996
40	40.0200	55	55.1800	0.2500	0.2496
60	59.5000	80	79.5300	0.3000	0.2996
80	79.9100	95	94.9300	0.3500	0.3496
100	100.6500	115	115.6700	0.4000	0.3996
120	117.8500	135	132.9500	0.4500	0.4496

In this section, simulation results are provided to demonstrate the performance of the proposed algorithm, in comparison with OPMUSIC [10] and TSMUSIC [12], where $d = \lambda/4$, all NF signals are of equal power σ_s^2 , and the signal to noise ratio (SNR) is defined as $10\log_{10}\left(\sigma_s^2/\sigma_w^2\right)$. Define the root-mean-square error (RMSE) of the value to be estimated from V Monte Carlo trials as: $RMSE = \sqrt{\frac{1}{KV}\sum_{v=1}^{V}\sum_{k=1}^{K}\left(\hat{x}_k^{(v)} - x_k\right)^2}$.

Example 1: *Performance test* - There are six uncorrelated NF sources impinging onto a symmetric cross array with $M_x = M_y = 1$, i.e., each ULA contains only 3 sensors and the total number of elements of the cross array is 5. The SNR, the number of snapshots N, the number of frames L and Monte Carlo trials are set to be 30dB, 1000, 100 and 50 respectively. The estimation result is shown in Table 1, where we can see that that all the DOAs of the six NF sources have been identified and paired correctly, showing that the proposed algorithm is working effectively for the underdetermined case.

Example 2: *RMSE versus SNR* - The performance of the proposed algorithm is studied with respect to SNR. There are three uncorrelated NF sources impinging onto a symmetric cross array with $M_x = M_y = 2$. The number of snapshots N, frames L and Monte Carlo trials are set to be 400, 50 and 500, respectively. From Fig. 2, we can see that the estimation performance of the proposed algorithm is better than the other two algorithms, especially for low SNR regions.

5. CONCLUSIONS

In this work, a new localization method for NF sources has been proposed using a cross array. It can realize 3-D parameter estimation for underdetermined case with automatic pairing, and as it does not require simultaneous multi-dimensional search, it has a low computational complexity. As demonstrated by computer simulations, it has outperformed the two existing representative algorithms.

6. REFERENCES

[1] Zhipeng Lin, Tiejun Lv, Wei Ni, J. Andrew Zhang, Jie Zeng, and Ren Ping Liu, "Joint estimation of multipath angles and delays for millimeter-wave cylindrical arrays

with hybrid front-ends," *IEEE Transactions on Wireless Communications*, vol. 20, no. 7, pp. 4631–4645, 2021.

[2] Junpeng Shi, Fangqing Wen, Yongxiang Liu, Qinmu Shen, Zhihui Li, and Zhen Liu, "Parameter identifiability of spatial-smoothing-based bistatic MIMO radar," in *ICASSP 2021 - 2021 IEEE International Conference on Acoustics, Speech and Signal Processing (ICASSP)*, 2021, pp. 4420–4424.

[3] Ye Tian, Wei Liu, He Xu, Shuai Liu, and Zhiyan Dong, "2-D DOA estimation of incoherently distributed sources considering gain-phase perturbations in massive MIMO systems," *IEEE Transactions on Wireless Communications*, pp. 1–1, 2021.

[4] Riheng Wu, Mei Wang, and Zhenhai Zhang, "Computationally efficient DOA and carrier estimation for coherent signal using single snapshot and its time-delay replications," *IEEE Transactions on Aerospace and Electronic Systems*, vol. 57, no. 4, pp. 2469–2480, 2021.

[5] Jisheng Dai and Hing Cheung So, "Real-valued sparse bayesian learning for DOA estimation with arbitrary linear arrays," *IEEE Transactions on Signal Processing*, vol. 69, pp. 4977–4990, 2021.

[6] Qisen Wang, Hua Yu, Jie Li, Fei Ji, and Fangjiong Chen, "Sparse bayesian learning using generalized double pareto prior for DOA estimation," *IEEE Signal Processing Letters*, vol. 28, pp. 1744–1748, 2021.

[7] Hua Chen, Weifeng Wang, and Wei Liu, "Joint DOA, range, and polarization estimation for rectilinear sources with a COLD array," *IEEE Wireless Communications Letters*, vol. 8, no. 5, pp. 1398–1401, 2019.

[8] A.L. Swindlehurst and T. Kailath, "Passive direction-of-arrival and range estimation for near-field sources," in *Fourth Annual ASSP Workshop on Spectrum Estimation and Modeling*, 1988, pp. 123–128.

[9] A.J. Weiss and B. Friedlander, "Range and bearing estimation using polynomial rooting," *IEEE Journal of Oceanic Engineering*, vol. 18, no. 2, pp. 130–137, 1993.

[10] Jin He, M. N. S. Swamy, and M. Omair Ahmad, "Efficient application of MUSIC algorithm under the coexistence of far-field and near-field sources," *IEEE Transactions on Signal Processing*, vol. 60, no. 4, pp. 2066–2070, 2012.

[11] Xiaofei Zhang, Weiyang Chen, Wang Zheng, Zhongxi Xia, and Yunfei Wang, "Localization of near-field sources: A reduced-dimension MUSIC algorithm," *IEEE Communications Letters*, vol. 22, no. 7, pp. 1422–1425, 2018.

[12] Junli Liang and Ding Liu, "Passive localization of mixed near-field and far-field sources using two-stage MUSIC algorithm," *IEEE Transactions on Signal Processing*, vol. 58, no. 1, pp. 108–120, 2010.

[13] Ke Deng and Qinye Yin, "Closed form parameters estimation for 3-D near field sources," in *2006 IEEE International Conference on Acoustics Speech and Signal Processing Proceedings*, 2006, vol. 4, pp. IV–IV.

[14] K. Abed-Meraim and Y. Hua, "3-D near field source localization using second order statistics," in *Conference Record of the Thirty-First Asilomar Conference on Signals, Systems and Computers (Cat. No.97CB36136)*, 1997, vol. 2, pp. 1307–1311 vol.2.

[15] Xiaohuan Wu and Wei-Ping Zhu, "Single far-field or near-field source localization with sparse or uniform cross array," *IEEE Transactions on Vehicular Technology*, vol. 69, no. 8, pp. 9135–9139, 2020.

[16] Raghu N. Challa and Sanyogita Shamsunder, "Passive near-field localization of multiple non-gaussian sources in 3-D using cumulants," *Signal Processing*, vol. 65, no. 1, pp. 39–53, 1998.

[17] Xiaohuan Wu and Jun Yan, "3-D mixed far-field and near-field sources localization with cross array," *IEEE Transactions on Vehicular Technology*, vol. 69, no. 6, pp. 6833–6837, 2020.

[18] Yang-Yang Dong, Chun-xi Dong, Zhi-bo Shen, and Guo-qing Zhao, "Conjugate augmented spatial temporal technique for 2-D DOA estimation with L-shaped array," *IEEE Antennas and Wireless Propagation Letters*, vol. 14, pp. 1622–1625, 2015.

[19] Hua Chen, Wei Liu, Wei-Ping Zhu, and M.N.S. Swamy, "Noncircularity-based localization for mixed near-field and far-field sources with unknown mutual coupling," in *2018 IEEE International Conference on Acoustics, Speech and Signal Processing (ICASSP)*, 2018, pp. 3236–3240.

[20] Marius Pesavento, Alex B. Gershman, and Kon Max Wong, "On uniqueness of direction of arrival estimates using rank reduction estimator (RARE)," in *2002 IEEE International Conference on Acoustics, Speech, and Signal Processing*, 2002, vol. 3, pp. III–3021–III–3024.

[21] Marius Pesavento, CF Mecklenbrauker, and JF Bohme, "Multidimensional rank reduction estimator for parametric MIMO channel models," *Eurasip Journal on Advances in Signal Processing*, vol. 2004, no. 9, pp. 1–10, 2004.